

# MergeUp-augmented Semi-Weakly Supervised Learning for WSI Classification

Mingxi Ouyang<sup>1\*</sup>, Yuqiu Fu<sup>1\*</sup>, Renao Yan<sup>1\*†</sup>, ShanShan Shi<sup>1</sup>, Xitong Ling<sup>1</sup>, Lianghui Zhu<sup>1†</sup>,  
Yonghong He<sup>1†</sup>, Tian Guan<sup>1†</sup>

<sup>1</sup>Tsinghua Shenzhen International Graduate School, Tsinghua University, China

## Abstract

Recent advancements in computational pathology and artificial intelligence have significantly improved whole slide image (WSI) classification. However, the gigapixel resolution of WSIs and the scarcity of manual annotations present substantial challenges. Multiple instance learning (MIL) is a promising weakly supervised learning approach for WSI classification. Recently research revealed employing pseudo bag augmentation can encourage models to learn various data, thus bolstering models' performance. While directly inheriting the parents' labels can introduce more noise by mislabeling in training. To address this issue, we translate the WSI classification task from weakly supervised learning to semi-weakly supervised learning, termed SWS-MIL, where adaptive pseudo bag augmentation (AdaPse) is employed to assign labeled and unlabeled data based on a threshold strategy. Using the "student-teacher" pattern, we introduce a feature augmentation technique, MergeUp, which merges bags with low-priority bags to enhance inter-category information, increasing training data diversity. Experimental results on the CAMELYON-16, BRACS, and TCGA-LUNG datasets demonstrate the superiority of our method over existing state-of-the-art approaches, affirming its efficacy in WSI classification.

## Introduction

In recent years, the combination of digital pathology and artificial intelligence has witnessed advanced progress. Whole slide image (WSI) classification has emerged as a fundamental clinical task for diagnosing various diseases (Yu et al. 2023; Raciti et al. 2023; Zhu et al. 2023; Zheng et al. 2024). However, WSIs pose unique challenges due to their gigapixel resolution and the memory limitations of current hardware, making them difficult to process like natural images (Kumar, Gupta, and Gupta 2020; Borowsky et al. 2020; Komura and Ishikawa 2018). Additionally, the limited availability of manual annotations necessitates the use of tiled patches from WSIs, translating the classification task from a supervised learning (SL) approach to a weakly supervised learning (WSL) approach.

Among all the weakly supervised learning methodologies, multiple instance learning (MIL) (Silva-Rodríguez,

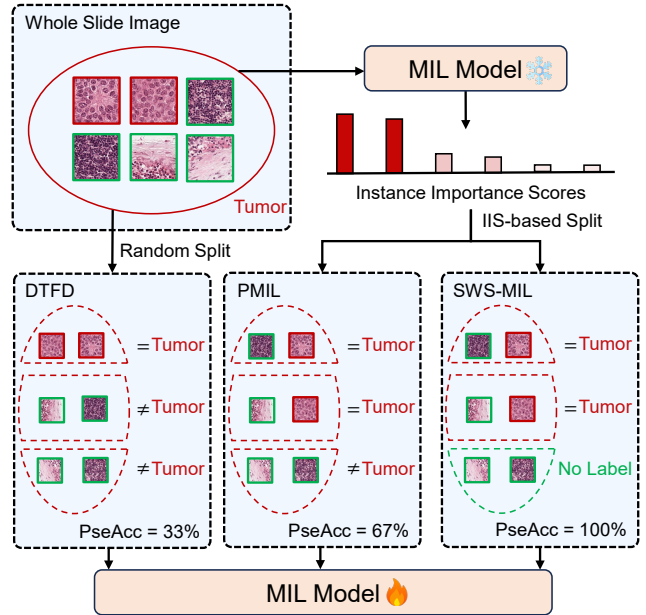


Figure 1: Mislabeling issue faced by different pseudo bag augmentation strategies.

Colomer, and Naranjo 2021; Jia et al. 2017; Wang et al. 2024) serves as a promising approach for WSI classification, where at least a positive instance in one bag marks the bag positive, otherwise negative. Current research in MIL focuses on extracting instance-level information from slide-level labels to enhance MIL training and fine-tune feature encoders. In attention-based MIL models, attention scores generated from attention pooling are used to estimate instance importance scores (IIS) (Yan et al. 2023). However, this approach is observed experimentally to overfitting due to the extreme distribution of attention scores.

To address this challenge, a notable strategy involves dividing regular bags into several pseudo bags, encouraging MIL models to learn from a greater variety of bags. As depicted in Figure 1, in existing pseudo bag-based approaches, the random split is commonly adopted, where each pseudo bag inherits its parent label. However, as the number of pseudo bags increases, more noise is introduced as an in-

\*These authors contributed equally to this work.

†Corresponding author.

creasing proportion of pseudo bags possess true labels that are inconsistent with their inherited labels. Note that the true labels of pseudo bags are unavailable, a common practice is to adjust the number of pseudo bags to find an optimal trade-off, aiming to maximize valid information from accurate pseudo labels while minimizing mislabeling noise (Yan et al. 2023). This rough strategy ties the NUMBER and LABEL assignment of pseudo bags, which is suboptimal since different WSIs have varying quantities of positive instances.

To overcome this limitation, we propose an adaptive pseudo bag assignment (AdaPse) method, which separates the number assignment and label assignment of pseudo bags, achieving a better trade-off point. In this approach, a threshold-based strategy is employed to filter out pseudo bags with high confidence. Pseudo bags whose predictions are inconsistent with their parent labels are discarded and recycled, while those with predictions consistent with their parent labels inherit their parent labels. The remaining pseudo bags with low confidence are left unlabeled. This method transforms the WSI classification task from a weakly supervised learning issue to a **semi-weakly supervised learning (SWSL)** issue.

Referring to semi-supervised learning (SSL), we adopt the “student-teacher” pattern (Tarvainen and Valpola 2017) as our main framework, applying the “weak and strong augmentation” strategy (Xie et al. 2020) for consistency regularization (Laine and Aila 2016). In computational pathology, feature augmentation is rarely studied, as most data augmentation techniques are unusable. Since the WSI classification task is based on one-hot labels, existing feature augmentation methods fail to capture the nuanced inclusion and exclusion relationships between categories, which is crucial when categories are not mutually exclusive, such as normal versus tumor, or cancer staging.

To address this issue, we propose a novel feature augmentation method, “MergeUp”, which merges different category bags while retaining the high-priority label, allowing models to learn the prioritization between different categories. In summary, our main contributions are as follows:

1. We propose a novel multiple instance learning framework SWS-MIL, where adaptive pseudo bag assignment, namely AdaPse is introduced for more reasonable pseudo augmentation, translating the weakly supervised learning task into a semi-weakly supervised learning task.

2. We introduce a feature augmentation method, MergeUp, to incorporate inter-category information into MIL training, which is suitable for non-mutually exclusive tasks and significantly increases the data diversity.

3. Extensive experiments on the CAMELYON-16, BRACS, and TCGA-LUNG datasets demonstrate that our method outperforms other state-of-the-art methods.

## Related Works

### Multiple Instance Learning

Current MIL models can be categorized into two types based on whether the final bag predictions are derived from direct instances (Avolio and Fuduli 2020; Gang, Yuan, and Bing 2013; Bernardini et al. 2020; Yang et al. 2023; Car-

bonneau, Granger, and Gagnon 2016) or the aggregated features of instances (Chen, Bi, and Wang 2006; Wang et al. 2018; Chen, Bi, and Wang 2006). ABMIL (Ilse, Tomczak, and Welling 2018) employed an attention mechanism to evaluate the contribution of each instance to the bag label. CLAM (Lu et al. 2021) utilized instance-level clustering to classify slides with slide-level labels. DTFD (Zhang et al. 2022) addressed the challenge of small sample cohorts in WSI classification by proposing pseudo bags to expand the number of bags and utilize intrinsic features. TransMIL (Shao et al. 2021) developed transformer-based attention to leveraging morphological and spatial information, thereby improving accuracy and convergence in WSI pathology diagnosis. PMIL (Yan et al. 2023) introduced Shapley values rather than attention scores to estimate the importance of each instance, achieving class-wise interpretation.

### Feature Augmentation

In deep learning, data augmentation is commonly used to improve generalization. However, most of these methods are not suitable for features under the MIL paradigm. Recently, MixUp (Zhang et al. 2017) has been introduced to MIL due to its strong adaptability. ReMix (Yang et al. 2022) proposed a “Mix-the-Bag” augmentation, which includes reducing and mixing. RankMix (Chen and Lu 2023) mixed ranked features from pairs of WSIs. PseMix (Liu et al. 2024) combined pseudo bag augmentation with the MixUp strategy. Although these methods attempted to introduce augmentation techniques from other fields into MIL, they overlooked the issue of non-mutual exclusivity between categories originating from clinical practice, resulting in soft labels from MixUp being illogical.

### Semi-supervised Learning

Semi-supervised learning aims to enhance models’ performance by leveraging large volumes of unlabeled data, commonly employing the “student-teacher” pattern and consistency regularization. Mean Teacher (Tarvainen and Valpola 2017) improved performance by averaging model weights instead of label predictions. UDA (Xie et al. 2020) introduced a “weak and strong augmentation” strategy for consistency regularization. FixMatch (Sohn et al. 2020) used a fixed high threshold (0.95) to ensure high-quality pseudo labels. FreeMatch (Wang et al. 2022) dynamically adjusted the confidence threshold and employed class fairness regularization to improve performance.

## Methods

In this section, we first review the MIL paradigm, then introduce various feature augmentation techniques, and finally propose our framework, as shown in Figure 2.

### MIL for WSI Classification

In this task, the input data, namely a set of labeled WSIs  $\mathcal{D} = \{X_i, Y_i\}_{i=1}^{|\mathcal{D}|}$ , are always tiled into  $N_i$  patches  $X_i = \{x_{i,j}\}_{j=1}^{N_i}$  for feature extraction. Conventionally, each instance  $x_{i,j}$  is extracted by a convolutional neural network

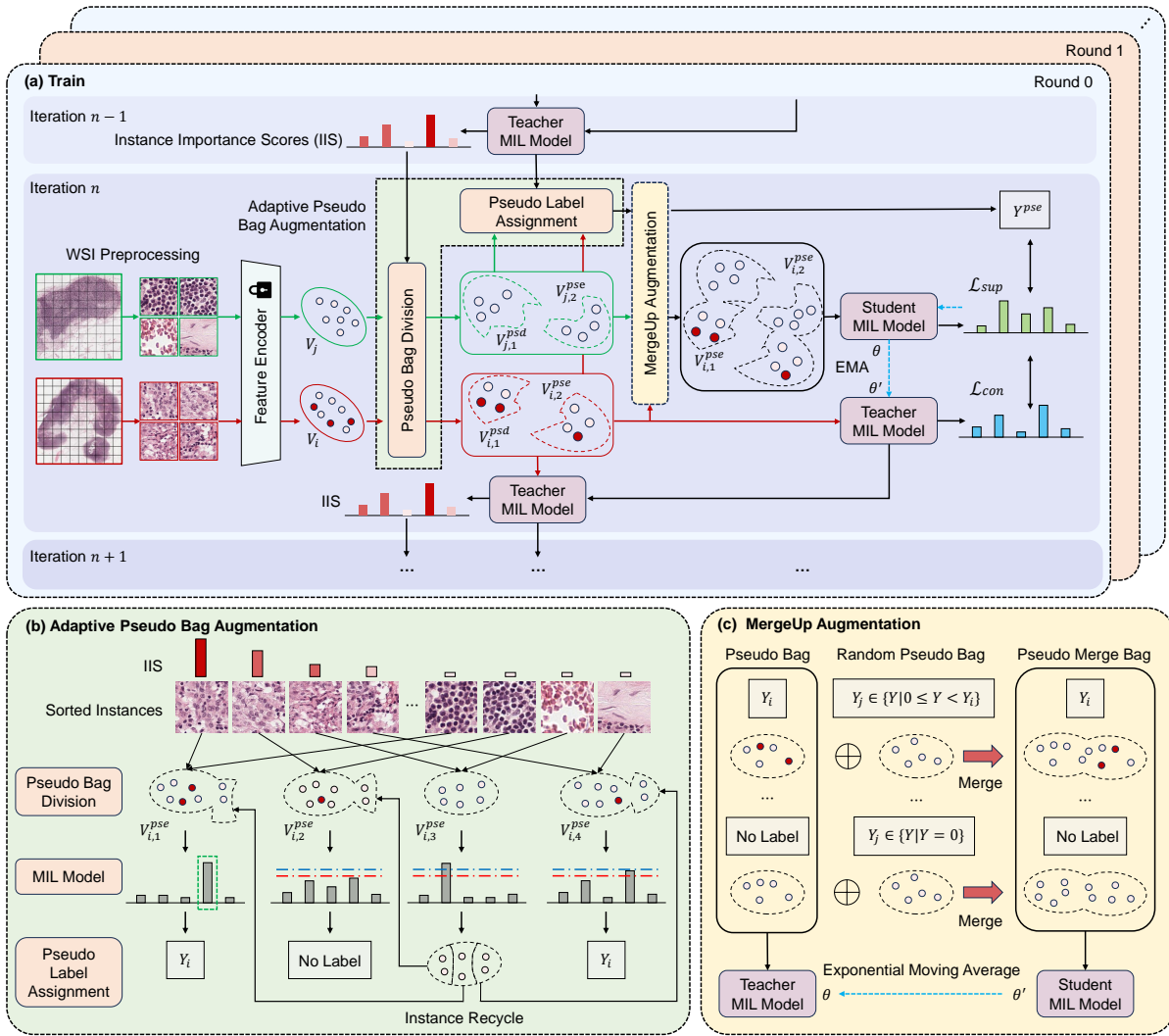


Figure 2: Overview of proposed semi-weakly supervised learning framework SWS-MIL. (a) All instances in WSIs are augmented by adaptive pseudo bags for the teacher model, and MergeUp augmentation is then applied for the student model. (b) Adaptive pseudo bag augmentation determines whether the pseudo bag label is correct and recycles the incorrectly labeled instances. (c) MergeUp augmentation blends instances from low-priority pseudo bags into high-priority pseudo bags.

$h(\cdot)$  to obtain the instance-level feature  $v_{i,j}$ :

$$v_{i,j} = h(x_{i,j}) \quad (1)$$

where the feature encoder  $h(\cdot)$  is usually frozen during training due to memory bottlenecks. All instance-level features in one bag will be aggregated for slide-level prediction  $\hat{Y}_i$  with confidence  $\gamma_i$ :

$$\hat{Y}_i = \max \gamma_i = \max \left\{ (f \circ g) \left( \{v_{i,j}\}_{j=1}^{N_i} \right) \right\}, \quad (2)$$

where  $g(\cdot)$  and  $f(\cdot)$  represent the aggregator and classifier.

### Feature Augmentation

During MIL training, the fixed nature of the feature encoder often leads to overfitting. To mitigate this issue, we introduce feature augmentation techniques.

**Adaptive Pseudo Bag.** One strategy to prevent the model from overfocusing on limited instances is to randomly split the bag  $V_i$  into  $M$  pseudo bags for training, denoted as:

$$V_i = \{v_{i,j}\}_{j=1}^{N_i} = V_{i,1}^{pse} \cup V_{i,2}^{pse} \cup \dots \cup V_{i,M}^{pse}. \quad (3)$$

Since the true pseudo bag label  $Y_{i,a}^{pse}$  is unavailable, each pseudo bag  $V_{i,a}^{pse}$  inherits the label  $Y_i$  from the parent bag, assigning  $\hat{Y}_{i,a}^{pse} = Y_i$ . This forms a pseudo bag dataset  $\mathcal{D}^{pse} = \{V_{i,a}^{pse}, \hat{Y}_{i,a}^{pse} = Y_i\}_{i=1}^{|\mathcal{D}|}$ ,  $a \in \{1, 2, \dots, M\}$ .

Random splitting can introduce significant label noise when  $\hat{Y}_{i,a}^{pse} \neq Y_i$ , which destabilizes training. To address this issue, progressively assigning pseudo bags based on IIS has been experimentally shown to be effective (Yan et al. 2023), where all instances in one bag are sorted in desc-

ing order of estimated IIS:

$$V'_i = \{v'_{i,j} \mid \text{IIS}(v'_{i,1}) \geq \text{IIS}(v'_{i,2}) \geq \dots \geq \text{IIS}(v'_{i,N_i})\} \quad (4)$$

Then these ordered instances are evenly interleaved into  $M$  pseudo bags:

$$V_{i,a}^{pse} = \left\{ v'_{i,(k-1)M+a} \right\}_{k=1}^{N_i/M}, a \in \{1, 2, \dots, M\}. \quad (5)$$

This approach can reduce noise generated by pseudo bag mislabeling to some extent. To take full advantage of pseudo bag augmentation, the number of pseudo bags  $M$  is usually set to a constant, which can be relatively large to extract more information from bags with many positive instances. However, in bags with only a few positive instances, the number of positive instances can be much lower than the given constant, where this framework cannot help.

To identify mislabeled pseudo bags, we freeze the training model’s parameters to provide predictions with confidence for each pseudo bag. Among all pseudo bags whose predictions are inconsistent with their parent labels, a fixed confidence threshold  $\gamma_{fix}$  is applied to filter out and discard those mislabeled pseudo bags, forming a discarded set  $\mathcal{D}_{dc}^{pse} = \left\{ V_{i,a}^{pse}, Y_i \mid \hat{Y}_{i,a}^{pse} \neq Y_i, \gamma_{i,a}^{pse} \geq \gamma_{fix} \right\}_{i=1}^{|\mathcal{D}|}$ ,  $a \in \{1, 2, \dots\}$  and a remaining set  $\mathcal{D}_{rm}^{pse} = \mathcal{D}^{pse} - \mathcal{D}_{dc}^{pse}$ .

To reuse these discarded mislabeled pseudo bags  $\left\{ V_{i,b}^{pse}, V_{i,c}^{pse}, \dots \right\} \in \mathcal{D}_{dc}^{pse}$ , we typically recycle these instances to the remaining pseudo bags  $V_{i,a}^{pse} \in \mathcal{D}_{rm}^{pse}$  evenly:

$$V_{i,b,a}^{pse} = \left\{ v_{i,b,(k-1)M+a}^{pse} \right\}_{k=1}^{|\mathcal{D}_{dc}^{pse}|/|\mathcal{D}_{rm}^{pse}|}, \quad (6)$$

$$V_{i,a}^{pse*} = V_{i,a}^{pse} \cup \left( V_{i,b,a}^{pse} \cup V_{i,c,a}^{pse} \cup \dots \right). \quad (7)$$

Then a new pseudo bag set  $\mathcal{D}^{pse*} = \left\{ V_{i,a}^{pse*}, Y_i \right\}_{i=1}^{|\mathcal{D}|}$ ,  $a \in \{1, 2, \dots\}$  is formed. For pseudo bags  $V_{i,a}^{pse} \in \mathcal{D}^{pse*}$  whose predictions match their parent labels, an adaptive confidence threshold  $\gamma_{ada}$  is applied to filter out and assign those highly confident pseudo bags their parent labels, denoted by:

$$\mathcal{D}_{lb}^{pse} = \left\{ V_{i,a}^{pse}, Y_i \mid \hat{Y}_{i,a}^{pse} = Y_i, \gamma_{i,a}^{pse} \geq \gamma_{ada} \right\}. \quad (8)$$

As the training model is initially cautious in prediction, we set the threshold  $\gamma_{ada}$  to a small constant and progressively increase it. The remaining pseudo bags are likely to contaminate the dataset, so they are treated unlabeled:

$$\mathcal{D}_{ulb}^{pse} = \left\{ V_{i,a}^{pse} \mid \hat{Y}_{i,a}^{pse} \neq Y_i, \gamma_{i,a}^{pse} < \gamma_{ada} \right\}. \quad (9)$$

Thus, the training set can be divided into a labeled pseudo bag set  $\mathcal{D}_{lb}^{pse}$  and an unlabeled one  $\mathcal{D}_{ulb}^{pse}$ , transforming weakly supervised learning into semi-weakly supervised learning and enhancing the diversity of training data.

**MergeUp.** In computational pathology, patches, and slides are prioritized in classification. For instance, in cancer subtyping, high-graded subtypes are typically more dominating than low-graded ones. It suggests that merging a

lower-priority bag retains the same slide-level label. In tumor detection, this can be interpreted as tumor bags remaining tumor regardless of how many normal bags are merged. Thus, the MergeUp augmentation can be represented as:

$$V_{i;j}^{mrg} = V_i \cup V_j, \quad (10)$$

$$Y_{i;j}^{mrg} = \max\{Y_i, Y_j\}. \quad (11)$$

## Semi-weakly Supervised Learning

We adopt the “student-teacher” pattern and “weak and strong augmentation” strategy in our framework. Formally, we regard identity as a “weak” augmentation for the teacher model and MergeUp as a “strong” augmentation for the student model, denoted by:

$$\hat{Y}_{i,a}^{pse,t} = (f^t \circ g^t)(V_{i,a}^{pse}), \quad (12)$$

$$\hat{Y}_{i,a;j,b}^{pse,s} = (f^s \circ g^s)(V_{i,a}^{pse} \cup V_{j,b}^{pse}), \quad (13)$$

where the superscripts  $t$  and  $s$  refer to teacher and student models. For unlabeled pseudo bags, they are trained by consistency loss between student and teacher models:

$$\mathcal{L}_{con} = \mathbb{E}_{f^t, g^t; f^s, g^s} \left[ \left\| \hat{Y}_{i,a}^{pse,t} - \hat{Y}_{i,a;j,b}^{pse,s} \right\|^2 \right]. \quad (14)$$

For labeled pseudo bags, they are trained by:

$$\mathcal{L}_{sup} = \mathcal{H}(\hat{Y}_{i,a}^{pse,s}, \bar{Y}_{i,a}^{pse}), \quad (15)$$

where  $\mathcal{H}(\cdot, \cdot)$  refers to the cross-entropy loss. The overall loss is then set to:

$$\mathcal{L} = \frac{1}{2} \mathcal{L}_{con} + \frac{1}{2} \mathcal{L}_{sup}. \quad (16)$$

## Experiences

### Datasets and Evaluation Metrics

**CAMELYON-16** is designed for detecting lymph node metastases in early-stage breast cancer. It consists of 399 WSIs, partitioned into 270 images for training and 129 for testing. We follow a 3-fold cross-validation protocol within the official training set, randomly selecting 20% as the validation set and using the remaining 80% for training.

**BRACS** (Brancati et al. 2022) is specifically curated for the nuanced task of breast cancer subtyping, serving as a critical resource for developing and evaluating automated classification systems. It comprises 547 WSIs, meticulously annotated for classification into three categories: benign tumors, atypical tumors (AT), and malignant tumors (MT). We follow a 3-fold cross-validation protocol, with the training/validation/test datasets set at a ratio of 7:1:2.

**TCGA-LUNG** includes 1,034 WSIs, comprising 528 cases of lung adenocarcinoma (LUAD) and 506 cases of lung squamous cell carcinoma (LUSC). We employ a 3-fold cross-validation protocol for both training and testing.

We utilized one-versus-others slide-level metrics: accuracy (ACC), the area under the curve (AUC), and macro F1 score (F1). We also introduced a new metric  $PseAcc$  to measure the pseudo label accuracy of pseudo bag assignment.

Table 1: Slide-level performance results on CAMELYON-16, BRACS and TCGA-LUNG. The subscripts are the standard deviation of each metric. The best evaluation results are in bold.

Method	CAMELYON-16			BRACS			TCGA-LUNG		
	ACC(%)	AUC(%)	F1(%)	ACC(%)	AUC(%)	F1(%)	ACC(%)	AUC(%)	F1(%)
MeanMIL	71.06 <sub>1.93</sub>	58.40 <sub>1.30</sub>	62.52 <sub>3.91</sub>	52.41 <sub>2.58</sub>	69.17 <sub>1.64</sub>	40.64 <sub>2.46</sub>	82.01 <sub>0.90</sub>	88.90 <sub>2.00</sub>	82.00 <sub>1.00</sub>
MaxMIL	83.98 <sub>1.59</sub>	87.98 <sub>0.99</sub>	81.75 <sub>1.86</sub>	55.86 <sub>2.78</sub>	75.88 <sub>1.61</sub>	50.29 <sub>4.02</sub>	88.70 <sub>1.00</sub>	94.40 <sub>1.20</sub>	88.70 <sub>1.00</sub>
DSMIL (Li, Li, and Eliceiri 2021)	77.52 <sub>1.68</sub>	76.76 <sub>1.27</sub>	74.43 <sub>2.72</sub>	53.10 <sub>2.20</sub>	70.82 <sub>3.30</sub>	46.10 <sub>3.71</sub>	86.20 <sub>1.40</sub>	93.60 <sub>1.00</sub>	86.20 <sub>1.40</sub>
ABMIL (Ilse, Tomczak, and Welling 2018)	83.21 <sub>0.97</sub>	84.60 <sub>0.55</sub>	81.33 <sub>0.88</sub>	58.39 <sub>0.86</sub>	76.14 <sub>0.64</sub>	54.74 <sub>2.29</sub>	87.60 <sub>0.70</sub>	93.10 <sub>1.80</sub>	87.60 <sub>0.70</sub>
CLAM (Lu et al. 2021)	84.50 <sub>2.19</sub>	83.37 <sub>0.90</sub>	82.50 <sub>2.27</sub>	53.79 <sub>3.52</sub>	73.25 <sub>1.65</sub>	51.50 <sub>3.29</sub>	88.20 <sub>1.40</sub>	94.20 <sub>1.20</sub>	88.20 <sub>1.40</sub>
TransMIL (Shao et al. 2021)	85.27 <sub>1.10</sub>	88.75 <sub>0.60</sub>	83.81 <sub>0.96</sub>	57.01 <sub>2.37</sub>	75.46 <sub>1.00</sub>	49.22 <sub>5.15</sub>	87.90 <sub>0.80</sub>	94.80 <sub>0.80</sub>	87.90 <sub>0.90</sub>
DTFD (Zhang et al. 2022)	84.76 <sub>1.83</sub>	84.82 <sub>3.94</sub>	84.45 <sub>1.93</sub>	57.24 <sub>2.66</sub>	76.55 <sub>1.99</sub>	56.20 <sub>3.76</sub>	88.80 <sub>0.60</sub>	94.60 <sub>0.80</sub>	88.80 <sub>0.60</sub>
R <sup>2</sup> T (Tang et al. 2024)	74.69 <sub>2.14</sub>	73.53 <sub>5.50</sub>	72.01 <sub>3.26</sub>	66.00 <sub>4.78</sub>	69.93 <sub>3.52</sub>	53.30 <sub>3.07</sub>	88.29 <sub>0.61</sub>	79.06 <sub>0.74</sub>	78.99 <sub>0.90</sub>
PMIL (Yan et al. 2023)	88.11 <sub>0.97</sub>	89.34 <sub>1.60</sub>	86.99 <sub>0.82</sub>	68.95 <sub>0.16</sub>	84.65 <sub>1.62</sub>	54.32 <sub>5.76</sub>	91.30 <sub>1.40</sub>	96.50 <sub>0.90</sub>	91.30 <sub>1.40</sub>
MixUp (Zhang et al. 2017)	66.93 <sub>2.72</sub>	75.29 <sub>1.72</sub>	66.23 <sub>2.40</sub>	30.38 <sub>10.46</sub>	55.77 <sub>1.90</sub>	53.20 <sub>5.60</sub>	66.83 <sub>2.66</sub>	71.32 <sub>2.83</sub>	64.96 <sub>4.08</sub>
AdditiveMIL (Javed et al. 2022)	67.27 <sub>6.10</sub>	56.40 <sub>3.40</sub>	59.58 <sub>4.80</sub>	54.25 <sub>2.60</sub>	74.18 <sub>0.50</sub>	47.37 <sub>1.90</sub>	80.95 <sub>3.60</sub>	88.25 <sub>1.40</sub>	80.83 <sub>3.80</sub>
RankMix (Chen and Lu 2023)	66.20 <sub>4.26</sub>	73.00 <sub>4.14</sub>	65.58 <sub>4.20</sub>	40.08 <sub>4.61</sub>	60.09 <sub>8.33</sub>	36.32 <sub>10.25</sub>	71.45 <sub>1.45</sub>	75.93 <sub>1.82</sub>	71.23 <sub>0.90</sub>
PseMix (Liu et al. 2024)	85.60 <sub>3.30</sub>	86.10 <sub>4.40</sub>	78.30 <sub>5.50</sub>	57.90 <sub>3.50</sub>	77.30 <sub>1.90</sub>	53.20 <sub>5.60</sub>	89.80 <sub>0.60</sub>	95.20 <sub>1.30</sub>	89.50 <sub>0.90</sub>
SWS-MIL (Shapley)	89.92 <sub>1.70</sub>	93.04 <sub>1.00</sub>	88.82 <sub>2.00</sub>	<b>69.80</b> <sub>1.50</sub>	<b>84.90</b> <sub>1.20</sub>	58.20 <sub>2.90</sub>	91.50 <sub>0.60</sub>	<b>97.00</b> <sub>0.60</sub>	91.40 <sub>0.60</sub>
SWS-MIL (Attention)	<b>90.18</b> <sub>1.60</sub>	<b>93.25</b> <sub>0.70</sub>	<b>89.27</b> <sub>1.70</sub>	69.40 <sub>4.00</sub>	84.40 <sub>1.50</sub>	<b>59.70</b> <sub>7.70</sub>	<b>91.60</b> <sub>0.50</sub>	96.80 <sub>0.70</sub>	<b>92.30</b> <sub>0.50</sub>

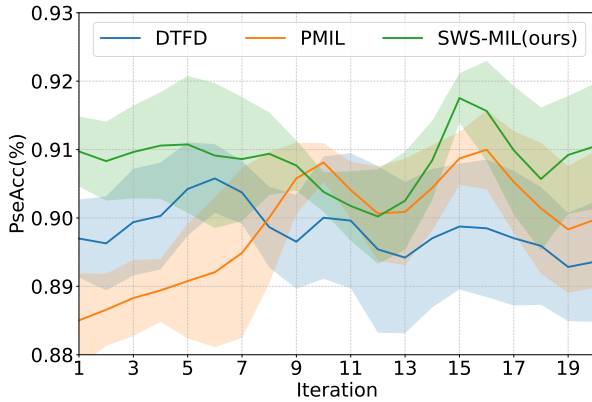


Figure 3: Pseudo label accuracy  $PseAcc$  of different pseudo bag augmentation methods during training.

## Implementation Details

We tiled non-overlapping  $256 \times 256$  pixel patches, at the magnification of  $5 \times$  for BRACS, and  $20 \times$  for CAMELYON-16, and TCGA-LUNG, resulting in average counts of 7156, 714, and 11951 patches per bag, respectively.

All experiments were conducted on a workstation equipped with NVIDIA RTX 4090 GPUs. We employed ResNet50 pretrained from the ImageNet dataset as the encoder and ABMIL as the primary MIL model. We implemented an early stopping strategy with the patience parameter set to 10 epochs. The initial learning rate was set to  $3e-4$  and was then reduced to  $1e-4$ . For the CAMELYON-16, BRACS, and TCGA-LUNG datasets, we set the maximum number of pseudo labels / bags to  $8 / 4$ ,  $10 / 6$ , and  $6 / 4$ .

The total number of training rounds was set to 10. We employed the same IIS estimation configuration for progressive pseudo bag augmentation (Yan et al. 2023).

## Evaluation and Comparison

We compared our performance on three datasets with various MIL methods, including Mean-Pooling MIL, Max-Pooling MIL, ABMIL (Ilse, Tomczak, and Welling 2018), DSMIL (Li, Li, and Eliceiri 2021), CLAM (Lu et al. 2021), TransMIL (Shao et al. 2021), DTFD (Zhang et al. 2022), R<sup>2</sup>T (Tang et al. 2024), and PMIL (Yan et al. 2023).

We also evaluated different feature-augmented methods, including MixUp (Zhang et al. 2017), AdditiveMIL (Javed et al. 2022), RankMix (Chen and Lu 2023), and PseMix (Liu et al. 2024).

As shown in Table 1, significant results were obtained in comparisons with both various MIL methods and different feature-augmented methods. In slide-level classification, SWS-MIL achieved AUC scores of 93.25%, 84.90%, and 97.00%, along with ACC scores of 90.18%, 69.80%, and 91.60% for the CAMELYON-16, BRACS, and TCGA-LUNG datasets, respectively, which outperformed other mainstream methods, highlighting the dynamic adaptability of our model.

To explain the inner mechanism for the high performance of our method, we reported the pseudo label accuracy of different pseudo bag assignment methods during training, as illustrated in Figure 3. It revealed that random splitting like DTFD introduces more noise than IIS-based splitting, where SWS-MIL performed better than PMIL as it alleviates the mislabeling issue to some extent.

## Visualization and Interpretation

To evaluate the effectiveness of our framework, we analyzed the heatmap of SWS-MIL for both macro and micro metastasis from CAMELYON-16, as shown in Figure 4 (a) and (b). In macro metastasis, our approach effectively avoids focusing on irrelevant fat or non-cancerous regions, which aligns with clinical annotations. In micro metastasis, our model accurately excludes regions labeled as normal in the ground truth, indicating that the model learns to characterize data more precisely.

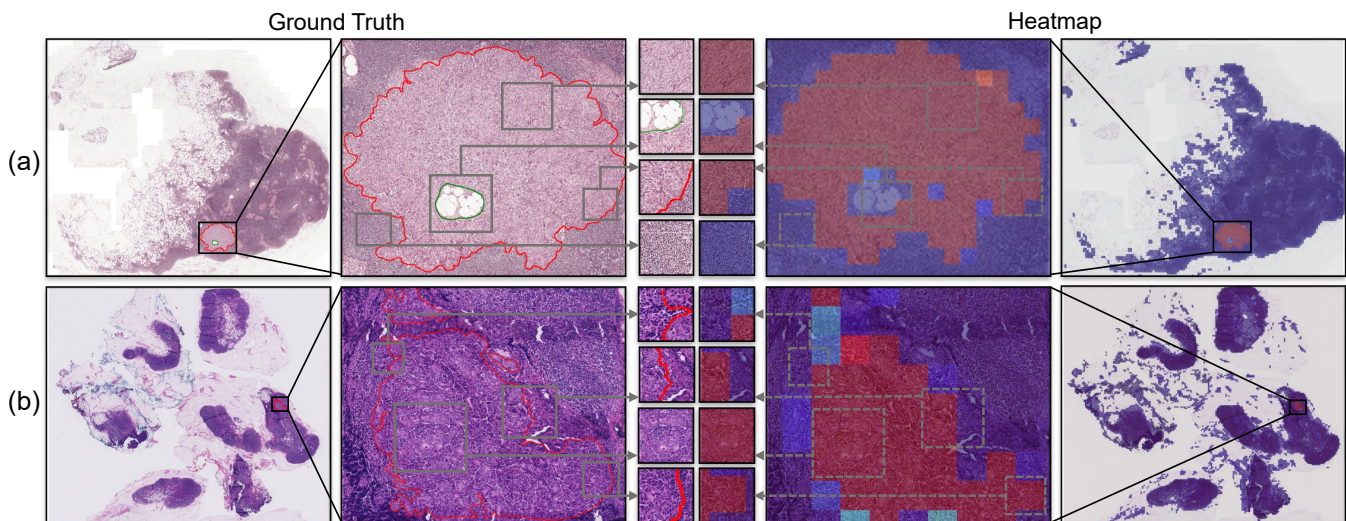


Figure 4: Heatmap of our method in the CAMELYON-16 dataset. (a) and (b) are macro and micro metastasis cases. In the column of "Ground Truth", cancer and non-cancer regions are delineated in red and green, respectively. The "Heatmap" column represents the prediction results of SWS-MIL, where a redder color indicates greater importance of instance.

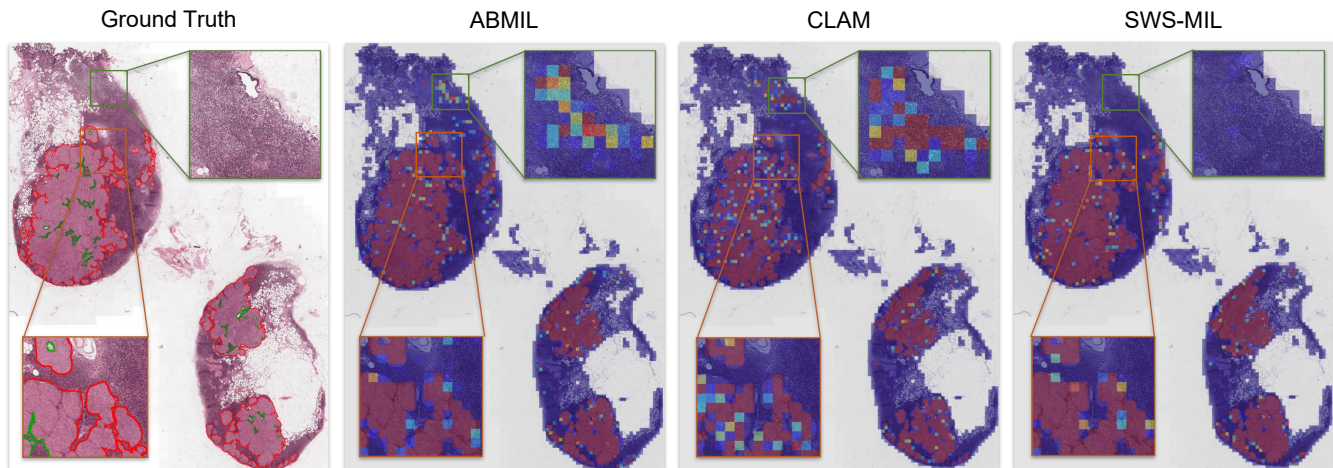


Figure 5: Heatmaps of a case from CAMELYON-16 generated by ABMIL, CLAM, and SWS-MIL respectively. In the "Ground Truth" column, tumor / normal regions are delineated by red / green lines. Brighter red colors indicate higher tumor probabilities.

Unlike weakly supervised learning frameworks, our semi-weakly supervised learning framework better utilizes inter-category information and optimizes pseudo label accuracy. As shown in Figure 5, SWS-MIL achieves more accurate and precise attention heatmaps compared with ABMIL and CLAM, especially in outline. Additionally, ABMIL and CLAM inevitably focus on some non-cancer regions while our model excludes nearly all non-cancer regions.

## Ablation Study

**Feature Augmentation Strategies.** We evaluated the effectiveness of MergeUp and AdaPse augmentation in subsequent training on CAMELYON-16, BRACS, and TCGA-LUNG datasets. For the "teacher" model, we adopt AdaPse

as the "weak augmentation". For the "student" model, we adopt MergeUp as the "strong augmentation".

From the ablation studies, we summarize two insights:

1. Adaptive confidence threshold is effective in improving pseudo bag labeling accuracy. As shown in Table 2, the performance of the model with AdaPse augmentation improved by 1% on both datasets compared to the baseline, especially on challenging BRACS. By setting adaptively adjusted pseudo bag label delineation thresholds, the model can better exclude incorrect labels and retain correct ones.

2. Hybrid augmentation strategy works out. We analyzed the impact of adding a feature augmentation method on model performance by comparing our proposed MergeUp with a hybrid effective feature augmentation strategy, as

Table 2: Ablation experiments of various augmentations on CAMELYON-16, BRACS and TCGA-LUNG. The subscripts are the standard deviation of each metric. The best evaluation results are in bold.

Augmentation		CAMELYON-16			BRACS			TCGA-LUNG		
Student	Teacher	ACC(%)	AUC(%)	F1(%)	ACC(%)	AUC(%)	F1(%)	ACC(%)	AUC(%)	F1(%)
/	/	87.44 <sub>2.80</sub>	89.70 <sub>0.70</sub>	86.26 <sub>2.70</sub>	66.79 <sub>1.72</sub>	84.37 <sub>1.57</sub>	55.24 <sub>2.62</sub>	91.20 <sub>1.00</sub>	96.40 <sub>0.70</sub>	91.20 <sub>1.10</sub>
/	AdaPse	88.11 <sub>1.61</sub>	89.05 <sub>4.06</sub>	86.92 <sub>1.79</sub>	67.54 <sub>3.42</sub>	<b>85.94</b> <sub>2.36</sub>	57.76 <sub>4.26</sub>	91.70 <sub>1.00</sub>	97.10 <sub>0.50</sub>	91.70 <sub>1.00</sub>
MergeUp	AdaPse	<b>90.18</b> <sub>1.60</sub>	<b>93.25</b> <sub>0.70</sub>	<b>89.27</b> <sub>1.70</sub>	<b>69.80</b> <sub>1.50</sub>	84.90 <sub>1.20</sub>	<b>58.20</b> <sub>2.90</sub>	<b>92.30</b> <sub>0.70</sub>	<b>97.20</b> <sub>0.50</sub>	<b>92.20</b> <sub>0.70</sub>

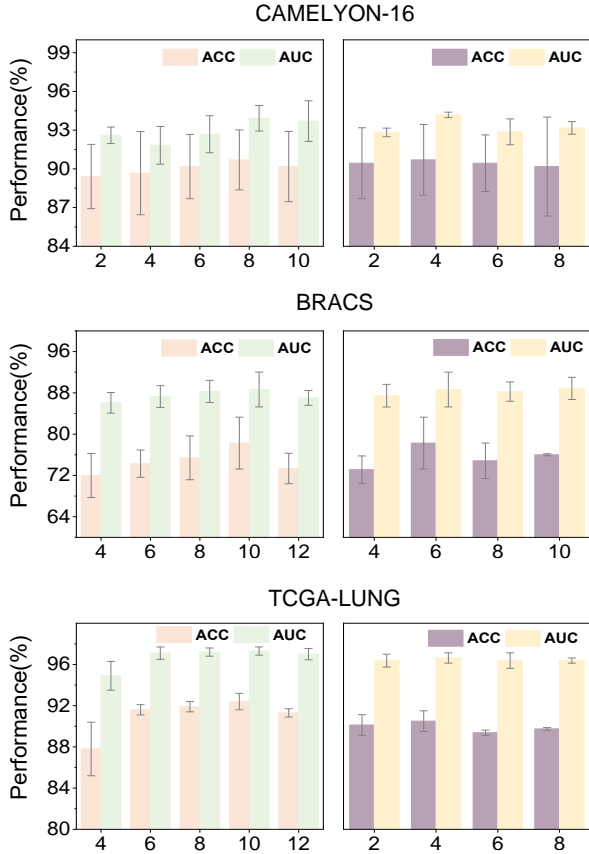


Figure 6: Performance of SWS-MIL over different numbers of pseudo labels and bags on CAMELYON-16, BRACS, and TCGA-LUNG datasets.

shown in Table 2. The inclusion of the MergeUp strategy led to performance improvements across nearly all metrics in the three datasets. Specifically, metrics for datasets CAMELYON-16 and BRACS improved by 2% compared to using only AdaPse, with dataset TCGA-LUNG also showing enhancements. The only exception was a slight decrease in the AUC metric for the dataset BRACS, and this may be attributed to the challenging nature of the BRACS dataset, which is sensitive to the setting of the pseudo bag.

**Hyper-parameter Analysis.** As illustrated in Figure 6, we evaluated two crucial hyper-parameters in SWS-MIL on the CAMELYON-16, BRACS, and TCGA-LUNG datasets: the

number of pseudo bags / pseudo labels. Based on our experimental results, the most suitable hyper-parameters are 8 / 4 for CAMELYON-16, 10 / 6 for BRACS, and 10 / 4 for TCGA-LUNG.

For the number of pseudo bags, the results show that the performance of SWS-MIL initially improves on both datasets with the increase in the number of bags, reaching the best value of 8 on CAMELYON-16 and 10 on BRACS and TCGA-LUNG, respectively, and then decreases. Similarly, the number of pseudo labels is evaluated, and the results show that the model performance improves as the number of labels increases from 2 to 10, reaching a peak of 4 on CAMELYON-16 and TCGA-LUNG, and 6 on BRACS.

Our conclusion combines the trends of the ACC and AUC metrics. In the ablation experiments on the BRACS and TCGA-LUNG datasets, while the accuracy of SWS-MIL fluctuates smoothly with the increase in the number of pseudo bags, the ACC significantly improves when the number of pseudo bags is set to 10. In contrast, in the ablation experiments on the number of pseudo labels on the CAMELYON-16 dataset, the ACC metric shows minimal fluctuations with the increase in the number of pseudo labels. However, when the number of pseudo-labels is set to 4, our model shows a clear advantage in AUC on CAMELYON-16.

## Conclusion

Our method can present a generalized approach to further improve the efficiency of MIL models by enhancing the efficiency of inter-category feature learning and digging out more information without adding additional data and annotations to the datasets. It achieved top performance in the verification experiments across the three datasets CAMELYON-16, BRACS, and TCGA-LUNG. Our method also demonstrated strong characteristics in the ablation experiments, and based on these results, we selected the optimal hyperparameters. It is worth noting that our experimental report indicated that the inherent mechanism of our excellent performance is attributed to accurate pseudo label allocation.

In future work, we will continue to compress the module size to increase training speed. We will explore inter-category feature fusion methods for mutually exclusive datasets in the future.

## References

- Avolio, M.; and Fuduli, A. 2020. A semiproximal support vector machine approach for binary multiple instance learning. *IEEE transactions on neural networks and learning systems*, 32(8): 3566–3577.
- Bernardini, M.; Morettini, M.; Romeo, L.; Frontoni, E.; and Burattini, L. 2020. Early temporal prediction of type 2 diabetes risk condition from a general practitioner electronic health record: a multiple instance boosting approach. *Artificial Intelligence in Medicine*, 105: 101847.
- Borowsky, A. D.; Glassy, E. F.; Wallace, W. D.; Kallichanda, N. S.; Behling, C. A.; Miller, D. V.; Oswal, H. N.; Feddersen, R. M.; Bakhtar, O. R.; Mendoza, A. E.; et al. 2020. Digital whole slide imaging compared with light microscopy for primary diagnosis in surgical pathology: a multicenter, double-blinded, randomized study of 2045 cases. *Archives of pathology & laboratory medicine*, 144(10): 1245–1253.
- Brancati, N.; Anniciello, A. M.; Pati, P.; Riccio, D.; Scognamiglio, G.; Jaume, G.; De Pietro, G.; Di Bonito, M.; Foncubierta, A.; Botti, G.; et al. 2022. Bracs: A dataset for breast carcinoma subtyping in h&e histology images. *Database*, 2022: baac093.
- Carbonneau, M.-A.; Granger, E.; and Gagnon, G. 2016. Witness identification in multiple instance learning using random subspaces. In *2016 23rd International Conference on Pattern Recognition (ICPR)*, 3639–3644. IEEE.
- Chen, Y.; Bi, J.; and Wang, J. Z. 2006. MILES: Multiple-instance learning via embedded instance selection. *IEEE transactions on pattern analysis and machine intelligence*, 28(12): 1931–1947.
- Chen, Y.-C.; and Lu, C.-S. 2023. Rankmix: Data augmentation for weakly supervised learning of classifying whole slide images with diverse sizes and imbalanced categories. In *Proceedings of the IEEE/CVF Conference on Computer Vision and Pattern Recognition*, 23936–23945.
- Gang, J.; Yuan, F.; and Bing, Z. 2013. Medical image semantic annotation based on MIL. In *2013 ICME International Conference on Complex Medical Engineering*, 85–90. IEEE.
- Ilse, M.; Tomczak, J.; and Welling, M. 2018. Attention-based deep multiple instance learning. In *International conference on machine learning*, 2127–2136. PMLR.
- Javed, S. A.; Juyal, D.; Padigela, H.; Taylor-Weiner, A.; Yu, L.; and Prakash, A. 2022. Additive mil: Intrinsically interpretable multiple instance learning for pathology. *Advances in Neural Information Processing Systems*, 35: 20689–20702.
- Jia, Z.; Huang, X.; Eric, I.; Chang, C.; and Xu, Y. 2017. Constrained deep weak supervision for histopathology image segmentation. *IEEE transactions on medical imaging*, 36(11): 2376–2388.
- Komura, D.; and Ishikawa, S. 2018. Machine learning methods for histopathological image analysis. *Computational and structural biotechnology journal*, 16: 34–42.
- Kumar, N.; Gupta, R.; and Gupta, S. 2020. Whole slide imaging (WSI) in pathology: current perspectives and future directions. *Journal of digital imaging*, 33(4): 1034–1040.
- Laine, S.; and Aila, T. 2016. Temporal ensembling for semi-supervised learning. *arXiv preprint arXiv:1610.02242*.
- Li, B.; Li, Y.; and Eliceiri, K. W. 2021. Dual-stream multiple instance learning network for whole slide image classification with self-supervised contrastive learning. In *Proceedings of the IEEE/CVF conference on computer vision and pattern recognition*, 14318–14328.
- Liu, P.; Ji, L.; Zhang, X.; and Ye, F. 2024. Pseudo-Bag Mixup Augmentation for Multiple Instance Learning-Based Whole Slide Image Classification. *IEEE Transactions on Medical Imaging*.
- Lu, M. Y.; Williamson, D. F.; Chen, T. Y.; Chen, R. J.; Barbieri, M.; and Mahmood, F. 2021. Data-efficient and weakly supervised computational pathology on whole-slide images. *Nature biomedical engineering*, 5(6): 555–570.
- Raciti, P.; Sue, J.; Retamero, J. A.; Ceballos, R.; Godrich, R.; Kunz, J. D.; Casson, A.; Thiagarajan, D.; Ebrahimzadeh, Z.; Viret, J.; et al. 2023. Clinical validation of artificial intelligence-augmented pathology diagnosis demonstrates significant gains in diagnostic accuracy in prostate cancer detection. *Archives of Pathology & Laboratory Medicine*, 147(10): 1178–1185.
- Shao, Z.; Bian, H.; Chen, Y.; Wang, Y.; Zhang, J.; Ji, X.; et al. 2021. Transmil: Transformer based correlated multiple instance learning for whole slide image classification. *Advances in neural information processing systems*, 34: 2136–2147.
- Silva-Rodríguez, J.; Colomer, A.; and Naranjo, V. 2021. WeGleNet: A weakly-supervised convolutional neural network for the semantic segmentation of Gleason grades in prostate histology images. *Computerized Medical Imaging and Graphics*, 88: 101846.
- Sohn, K.; Berthelot, D.; Carlini, N.; Zhang, Z.; Zhang, H.; Raffel, C. A.; Cubuk, E. D.; Kurakin, A.; and Li, C.-L. 2020. Fixmatch: Simplifying semi-supervised learning with consistency and confidence. *Advances in neural information processing systems*, 33: 596–608.
- Tang, W.; Zhou, F.; Huang, S.; Zhu, X.; Zhang, Y.; and Liu, B. 2024. Feature Re-Embedding: Towards Foundation Model-Level Performance in Computational Pathology. *arXiv preprint arXiv:2402.17228*.
- Tarvainen, A.; and Valpola, H. 2017. Mean teachers are better role models: Weight-averaged consistency targets improve semi-supervised deep learning results. *Advances in neural information processing systems*, 30.
- Wang, X.; Shi, S.; Yan, R.; Sun, Q.; Zhu, L.; Guan, T.; and He, Y. 2024. Task-oriented Embedding Counts: Heuristic Clustering-driven Feature Fine-tuning for Whole Slide Image Classification. *arXiv preprint arXiv:2406.00672*.
- Wang, X.; Yan, Y.; Tang, P.; Bai, X.; and Liu, W. 2018. Revisiting multiple instance neural networks. *Pattern Recognition*, 74: 15–24.
- Wang, Y.; Chen, H.; Heng, Q.; Hou, W.; Fan, Y.; Wu, Z.; Wang, J.; Savvides, M.; Shinzaki, T.; Raj, B.; et al. 2022. Freematch: Self-adaptive thresholding for semi-supervised learning. *arXiv preprint arXiv:2205.07246*.



Xie, Q.; Dai, Z.; Hovy, E.; Luong, T.; and Le, Q. 2020. Un-supervised data augmentation for consistency training. *Advances in neural information processing systems*, 33: 6256–6268.

Yan, R.; Sun, Q.; Jin, C.; Liu, Y.; He, Y.; Guan, T.; and Chen, H. 2023. Shapley Values-enabled Progressive Pseudo Bag Augmentation for Whole Slide Image Classification. *arXiv preprint arXiv:2312.05490*.

Yang, B.; He, Y.; Jiao, C.; Pan, X.; Wang, G.; Wang, L.; and Wu, J. 2023. Multiple Instance Metric Learning Network for Hyperspectral Target Detection. *IEEE Transactions on Geoscience and Remote Sensing*.

Yang, J.; Chen, H.; Zhao, Y.; Yang, F.; Zhang, Y.; He, L.; and Yao, J. 2022. Remix: A general and efficient framework for multiple instance learning based whole slide image classification. In *International Conference on Medical Image Computing and Computer-Assisted Intervention*, 35–45. Springer.

Yu, J.-G.; Wu, Z.; Ming, Y.; Deng, S.; Li, Y.; Ou, C.; He, C.; Wang, B.; Zhang, P.; and Wang, Y. 2023. Prototypical multiple instance learning for predicting lymph node metastasis of breast cancer from whole-slide pathological images. *Medical Image Analysis*, 85: 102748.

Zhang, H.; Cisse, M.; Dauphin, Y. N.; and Lopez-Paz, D. 2017. mixup: Beyond empirical risk minimization. *arXiv preprint arXiv:1710.09412*.

Zhang, H.; Meng, Y.; Zhao, Y.; Qiao, Y.; Yang, X.; Coup-land, S. E.; and Zheng, Y. 2022. Dtf-d-mil: Double-tier feature distillation multiple instance learning for histopathology whole slide image classification. In *Proceedings of the IEEE/CVF Conference on Computer Vision and Pattern Recognition*, 18802–18812.

Zheng, R.; Wang, X.; Zhu, L.; Yan, R.; Li, J.; Wei, Y.; Zhang, F.; Du, H.; Guo, L.; He, Y.; et al. 2024. A Deep Learning Method for Predicting The Origins of Cervical Lymph Node Metastatic Cancer on Digital Pathological Images. *iScience*.

Zhu, L.; Shi, H.; Wei, H.; Wang, C.; Shi, S.; Zhang, F.; Yan, R.; Liu, Y.; He, T.; Wang, L.; et al. 2023. An accurate prediction of the origin for bone metastatic cancer using deep learning on digital pathological images. *EBioMedicine*, 87.